Received: 5 August 2024 | Accepted: 13 December 2024

DOI: 10.1097/HC9.0000000000000658

ORIGINAL ARTICLE

OPEN

A novel KEAP1 inhibitor, tiliroside, activates NRF2 to protect against acetaminophen-induced oxidative stress and acute liver injury

Fangfang Cai[1] | **Kaiqian Zhou**[2] | **Peipei Wang**[2] | **Wen Zhang**[3] | **Lei Liu**[4] | **Yunwen Yang**[2]

[1]Department of Cell Biology, School of Basic Medical Sciences, Nanjing Medical University, Nanjing, China

[2]Nanjing Key Laboratory of Pediatrics, Children's Hospital of Nanjing Medical University, Nanjing, China

[3]Department of Nephrology, Affiliated Hospital of Integrated Traditional Chinese and Western Medicine, Nanjing University of Chinese Medicine, Nanjing, China

[4]Department of Central Laboratory, Shaanxi Provincial People's Hospital, Beilin District, Xi'an, China

Correspondence
Yunwen Yang, Nanjing Key Laboratory of Pediatrics, Children's Hospital of Nanjing Medical University, 72 Guangzhou Road, Nanjing 210008, China.
Email: yangyunwen@njmu.edu.cn

Abstract

Background: Acetaminophen-induced acute liver injury (AILI) is one of the common causes of abrupt liver failure in numerous nations. Several previous studies revealed that tiliroside, a glycoside flavonoid, exerts neuroprotective and renal protective effects. However, whether it has hepatoprotective effects is not known. The objective of this research is to examine whether tiliroside can protect against AILI.

Methods: AILI mouse and cell models were performed to evaluate the protective effects of tiliroside. Molecular docking, cellular thermal shift assay, immunoprecipitation, and RNA-seq were performed to analyze the possible mechanisms of tiliroside.

Results: In vivo, tiliroside attenuated AILI in mice significantly, as evidenced by lower ALT and AST levels. Molecular docking, cellular thermal shift assay, and RNA-seq analysis revealed that tiliroside promoted the activation of nuclear factor erythroid 2-related factor 2 (NRF2) and the expression of its downstream genes through disruption of the NRF2-KEAP1 protein-protein interaction to inhibit KEAP1-mediated ubiquitination and degradation of NRF2, thereby inhibiting oxidative stress in the livers of AILI mice. Furthermore, hepatocyte-specific knockout of NRF2 greatly attenuated the hepatic-protective effects of tiliroside in mice. In vitro, tiliroside protected against acetaminophen-induced oxidative stress on cultured hepatocytes through activation of NRF2. In addition, NRF2 knockout markedly blunted the protection effects of tiliroside, suggesting that NRF2 mediates the hepatic-protective effects of tiliroside.

Abbreviations: 4-HNE, 4-hydroxynonenal; AILI, APAP-induced liver injury; APAP, acetaminophen; GPX4, glutathione peroxidase 4; GSH, glutathione; GSSG, glutathione disulfide; MDA, malondialdehyde; NRF2, nuclear factor erythroid 2-related factor 2; PPI, protein-protein interaction; ROS, reactive oxygen species; TUNEL, terminal deoxynucleotidyl transferase-mediated dUTP nick-end labeling.

Supplemental Digital Content is available for this article. Direct URL citations are provided in the HTML and PDF versions of this article on the journal's website, www.hepcommjournal.com.

Conclusions: Our study demonstrated that tiliroside could protect against AILI by activating the KEAP1/NRF2 pathway, which primarily inhibits the processing of oxidative stress and cell death. Our results suggest that tiliroside could serve as a potential agent for the clinical treatment of AILI.

Keywords: AILI, KEAP1, NRF2, oxidative stress, tiliroside

INTRODUCTION

Acetaminophen (APAP) is one of the most common analgesic and antipyretic drugs used worldwide. However, an overabundance of APAP can cause hepatocytes in the hepatic lobule to necrotize, which can result in severe acute liver failure.[1,2] *N*-acetyl-p-benzoquinone imine is the principal metabolite of APAP in hepatocytes.[3] Glutathione (GSH) conjugation is a detoxification method for *N*-acetyl-p-benzoquinone imine. Acute liver injury and hepatocyte death, on the other hand, are caused by the overabundance of *N*-acetyl-p-benzoquinone imine, which causes hepatic GSH depletion, leading to an overabundance of reactive oxygen species (ROS) production and mitochondrial dysfunction.[2,4] APAP overdose accounts for ~46% of drug-induced liver damage.[5] *N*-acetylcysteine (NAC) is the only drug that has been approved to treat acute liver injury. Nonetheless, NAC needs to be administered within 8 hours of APAP ingestion, and there is a restricted therapeutic window.[6] There are adverse reactions, such as allergic reactions and fluid overload.[7] Even within the recommended dose range, some patients will experience liver damage. In addition, the efficacy of NAC on APAP-induced liver inflammation is still unclear.[8] Therefore, the search for new and more effective therapeutic approaches is urgent.

Oxidative stress significantly contributes to APAP-induced hepatotoxicity. Mitigating oxidative stress is regarded as a promising approach for the treatment of APAP-induced acute liver injury (AILI).[9,10] NRF2 (nuclear factor erythroid 2-related factor 2) is a key intracellular antioxidant that fights oxidative stress in cells. NRF2 combines with promoters containing antioxidant response elements to enhance cellular antioxidant capacity by activating downstream gene transcription, such as that of antioxidant enzymes (superoxide dismutase, GSH) and detoxification molecules when cellular oxidative stress occurs.[11,12] To avoid unnecessarily activating these defense genes, ubiquitin-mediated proteasome degradation normally maintains low NRF2 protein levels.[13,14] The ubiquitination of NRF2 is catalyzed by Kelch-like ECH-associated protein 1 (KEAP1), the adaptor protein for NRF2. Oxidative stress causes KEAP1's cysteine residues to oxidize, which causes NRF2 to dissociate and stabilize NRF2. The expression of NRF2's downstream genes is then triggered when it enters the nucleus.[13,15] It has been proposed that targeting the NRF2 signaling axis is used to treat liver disease.[16–18] Consequently, a workable prospective target to mitigate APAP-induced hepatotoxicity is activating the NRF2 signaling pathway.

Notably, many natural compounds have shown efficacy in alleviating liver disease, and their active ingredients have hepatoprotective effects to some extent.[19,20] Accordingly, natural products capable of activating the NRF2 signaling pathway are potential resources for the development of therapeutic APAP overdose treatments. Several edible plants, including *Rosaceae* and certain plant parts (roots, fruits, or leaves), contain a kind of glycoside flavonoid called tiliroside.[21] Previous research has demonstrated that by activating AMP-activated protein kinase (AMPK), tiliroside, which possesses antioxidant, antihyperglycemic, and anti-inflammatory properties, can improve insulin resistance in diet-induced obese mice.[22–24] Through NRF2 activation, tiliroside and its derivatives have been demonstrated in recent research to protect nerves and have anti-neuroinflammatory actions.[23–25] Recently, we found tiliroside protects against acute kidney injury through NRF2 activation.[26] However, it is yet unclear if tiliroside protects against acute liver injury, so more research is required. In this study, we aimed to assess whether tiliroside affords protection against AILI in vivo and in vitro.

METHODS

Cell culture and treatment

The Transformed Human Liver Epithelial-2 cell line (THLE-2) , a well-established normal human hepatocyte cell line, was obtained from the Chinese Academy of Sciences Cell Bank. APAP was acquired from Aladdin in Shanghai, China, with a purity $>$ 99.99%. Tiliroside, with a purity of 99.78%, was obtained from APExBIO (N2081). Various levels of tiliroside (suspended in DMSO) were applied to cells for 1 hour once cell density reached around 60%–70%. Following that, a concentration of 10 mM APAP was introduced into the medium where the cells were then left to incubate for a period of 24 hours.

NRF2-knockout cells

CRISPR/Cas9 gene-editing method was used to create NRF2-knockout cells, as previously reported in the literature.[27] In summary, NRF2 sgRNAs were cloned and put into the PX458 vector (Addgene plasmid #48138) using the sequences indicated in Supplemental Table S1, http://links.lww.com/HC9/B908. The NRF2 sgRNA plasmids were introduced into cells, followed by sorting GFP-positive cells using flow cytometry. The successful knockout of NRF2 was confirmed by western blotting.

Animal models

Male C57BL/6 mice, around 6-8 weeks of age, were purchased from GemPharmatech in Nanjing, China. They were kept in a laboratory setting with a 22 ± 1°C temperature and a 12-hour light/dark cycle. Animals were given 5, 10, 20, or 30 mg/kg of tiliroside (dissolved in 0.5% methylcellulose) or vehicle daily by gavage for 48 hours, after which the animals were sacrificed to test whether tiliroside activated NRF2 in the liver. Seven groups of mice (n = 6) were randomly assigned to investigate the effect of tiliroside in the APAP-induced AILI mouse model: vehicle, tiliroside (20 mg/kg/d), tiliroside (30 mg/kg/d), vehicle + APAP (400 mg/kg), tiliroside (10 mg/kg/d) + APAP (400 mg/kg), tiliroside (20 mg/kg/d) + APAP (400 mg/kg), and tiliroside (30 mg/kg/d) + APAP (400 mg/kg). As Figure 2A illustrates, vehicle or tiliroside was administered daily by gavage to the mice. Mice were fasted overnight before i.p. injection of APAP. Blood samples and liver tissues were obtained 24 hours after the APAP injection for further analysis. The serum ALT and AST levels were determined in accordance with the manufacturer's instructions using a reagent kit. The Institutional Animal Care and Use Committee of Nanjing Medical University accepted the ARRIVE criteria, which were followed in all animal welfare and experimental operations.

Generation of hepatocyte-specific NRF2 knockout mice

To create hepatocyte-specific Cas9 expression mice, Rosa26-floxed STOP-CRISPR/Cas9 knock-in mice were crossed with Albumin-Cre mice, as previously reported.[28] The successful hepatocyte-specific NRF2 knockout mice were generated by i.v. injection of lentivirus carrying NRF2-sgRNA (Supplemental Table S1, http://links.lww.com/HC9/B908, displays the sequences). We simultaneously injected lentivirus carrying an empty vector into hepatocyte-specific Cas9 transgenic mice to serve as a control. For the ensuing tests, male knockout mice aged 6-8 weeks were acquired.

Cell viability

The Cell Counting Kit-8 (CCK8) test was used to measure the vitality of the cells. After treatment, 10 μL of CCK8 reagent (Sigma) was added to the medium, and it was incubated for 1–2 hours. The Titertek Multiskan MCC/340 microplate spectrophotometer was used to measure the optical density at a wavelength of 450 nm.

Real-time quantitative PCR assay

Total RNA was extracted from either raw liver tissues or cultivated cells using TRIzol (Invitrogen). In addition, qRT-PCR was carried out as follows: 45 seconds at 95°C and 1 minute at 55°C with 35-40 amplification cycles. 95°C was used to construct the melting curve, and then 65°C. Using the $2^{-\Delta\Delta CT}$ method, the target genes' relative mRNA levels were ascertained and calibrated against the loading control actin levels (Supplemental Table S1, http://links.lww.com/HC9/B908, lists all the primers).

Protein preparation and immunoblotting

The protocol for western blotting was followed by other studies.[29] To summarize, Radio Immunoprecipitation Assay lysis buffer mixed with 1 mM Phenylmethanesulfonyl fluoride was used to collect and homogenize liver tissues and THLE-2 cells. Antibodies included anti-NRF2 (Proteintech, 16396-1-AP), anti-Lamin B1 (Proteintech, 12987-1-AP), anti-MPO (RD, AF3667), anti-KEAP1 (Proteintech, 60027-1-Ig), anti-GPX4 (Proteintech, 14432-1-AP), anti-Cas9 (Cell Signaling Technology, 19526), and anti-β-actin (Proteintech, 66009-1-Ig). The membranes were observed using a Tannon ChemDoc imaging system in China the day after they had been washed 3 times with tris-buffered saline with tween 20 and subjected to secondary antibodies conjugated to horseradish peroxidase for 1 hour.

Protein ubiquitination assay

Cells were treated with the proteasome inhibitor MG132 (20 μM) for 6 hours after being exposed to either a vehicle or tiliroside (5 μM) for 24 hours. Cells were collected and lysates were then extracted with protein lysis buffer. Overnight at 4°C, 1 mg of isolated total protein was combined with NRF2 antibody. The next day, the cell lysates were treated with protein A/G agarose beads (sc-2003, Santa) for 2 hours at 4°C.

After additional washing, the samples were boiled in a sodium dodecyl sulfate-loading buffer to prepare them for western blot analysis.

The cellular thermal shift assay

To investigate tiliroside's direct binding to KEAP1, as reported in an earlier investigation,[30] cellular thermal shift assay was carried out. In summary, cells were subjected to treatment with either vehicle or tiliroside (5 μM), and then they were resuspended in PBS. Separating the suspension into equal aliquots (2×10^6 cells/aliquot), each was heated for 3 minutes at a different temperature (42, 44, 46, 48, 50, and 52°C). After adding 0.5% NP-40 and a protease inhibitor, freeze-thaw cycles were used to lyse the cells. Western blotting was used to evaluate the supernatants.

Histology and staining with TUNEL

Hematoxylin and eosin staining was used to visualize the histological damage in the mouse livers. To summarize, liver tissues were sectioned into 4 μm-thick slices, embedded in paraffin, fixed with 4% paraformaldehyde, and stained with hematoxylin and eosin. Following the manufacturer's instructions, a TUNEL BrightGreen detection kit (Vazyme) was used to visualize the APAP-induced cell death in liver tissues.

Immunohistochemistry

Sections of the liver (4 μm thick) were hydrated, blocked, and deparaffinized. The liver slices were then treated with antibodies against NRF2 (Proteintech, 16396-1-AP, 1:100) or 4-HNE (R&D Systems, MAB3249-SP, 1:150) for 12 hours at 4°C. The following day, the liver slices were washed 3 times with Tris-Buffered Saline with Tween before being incubated for 1 hour with a horseradish peroxidase–conjugated secondary antibody. Using a DAB kit (Zsbio, ZLI-9018), the liver slices were stained. Every segment was examined, and pictures were captured using a Carl Zeiss optical microscope. For quantification, 4–5 random immunohistochemistry images of each mouse were selected and analyzed by ImageJ (1.51) according to a previous study.[31]

Immunofluorescence staining

After being seeded on a 12-well culture plate using cell slides, cells were fixed in 4% paraformaldehyde for 20 minutes at room temperature (RT). Utilizing 0.1% Triton X-100, the cells were made permeable. The slides were then stained with anti-NRF2 (Proteintech, 16396-1-AP, 1:100) antibody for a whole night at 4°C. The nuclei were costained with DAPI (Beyotime, P0131), and the next day, the slides were incubated with a secondary antibody (Thermo Fisher Scientific Inc., #A21207) tagged for Alexa Fluor 488. Pictures were taken with a Zeiss LSM710 confocal microscope (Carl Zeiss).

Transmission electron microscopy

The liver tissues from the mice that received different treatments were analyzed by using a transmission electron microscope according to a standard method. For every sample, the proportion of damaged mitochondria was measured across 5 randomized fields of view.

MDA, GSH, and GSSG detection

By first homogenizing the collected liver tissues in PBS and then centrifuging the mixture to extract the supernatant. The MDA detection kit's instructions were followed to quantify the malondialdehyde (MDA) levels in the collected supernatant (Beyotime, S0131). The levels of oxidized glutathione disulfide (GSSG) and GSH in liver tissues or THLE-2 cells were evaluated using a GSH/GSSG Assay Kit (Beyotime, S0053). The manufacturer's instructions were followed for every experimental operation.

Mitochondria ROS

MitoSOX Red Mitochondrial Superoxide Indicator (Thermo Fisher, M36009), a specialized probe for the detection of superoxide in mitochondria, was used to quantify the generation of ROS in human hepatocyte (THLE-2 cells) mitochondria. After being subjected to tiliroside (5 μM) or APAP (10 mM) for a full day, cells were stained with the MitoSOX probe for 45 minutes at 37°C in the absence of light. After that, the nuclei were stained with Hoechst 33342, and images were captured using confocal microscopy.

Mitochondrial membrane potential

Tetramethylrhodamine methyl ester (Thermo Fisher, I34361) was incubated for 40 minutes at 37°C on THLE-2 cells treated with tiliroside (5 μM) or APAP (10 mM) to measure the mitochondrial membrane potential ($\Delta\Psi m$). Following that, confocal microscopy (LSM710, Carl Zeiss) was used to observe the cells.

Lipid peroxidation analysis

Thermo Fisher Scientific (D3861) C11-BODIPY 581/591 probe was utilized to examine APAP-induced lipid peroxidation in THLE-2 cells. Following seeding on confocal microscopy dishes, cells were exposed to tiliroside (5 μM) or APAP (10 mM) for a duration of 24 hours. The cells were then treated for 45 minutes at 37°C in the dark with the C11-BODIPY 581/591 probe (5 μM). An LSM710 confocal microscope (Carl Zeiss) was used to view the labeled cells' oxidized lipid peroxide.

RNA sequencing analysis

Mice in 3 groups were used for the liver collection: the vehicle group, the APAP + vehicle group, and the APAP + tiliroside group. LC-Bio Technologies (Hangzhou) carried out the sequencing analysis, appropriate library creation, and RNA isolation. Combining the OmicStudio tools provided at https://www.omicstudio.cn with a range of bioinformatics approaches, such as heatmap analysis, KEGG pathway enrichment analysis, and Gene Set Enrichment Analysis, allowed for the completion of further research. The NCBI SRA database received the mouse hepatic RNA-sequencing data under accession number PRJNA1017907.

Molecular docking

The Protein Data Bank (the code: 1U6D) provided the structure of KEAP1, which served as the basis for the molecular docking simulations carried out by the AutoDock Vina software. To utilize as a ligand, tiliroside's 3D structure was acquired from PubChem. KEAP1 and tiliroside underwent the conventional docking procedure with AutoDock Vina software. The London dG scoring function was applied to all docked positions, and the "induced fit" method was employed. The postures were then rescored using the GBVI/WSA dG scoring function. It was discovered that the conformation with the lowest free binding energy was the ideal binding mode. KEAP1 and tiliroside binding modes were shown using PyMOL (https://www.pymol.org).

Analytical statistics

The mean ± SD is used to express the data. The 2 groups were compared using the unpaired Student *t* test. To find significant differences across different groups, 1- or 2-way ANOVA was carried out using GraphPad Prism 9.0 (GraphPad). $p < 0.05$ was deemed significant.

RESULTS

Tiliroside activated the NRF2/ARE pathway both in vivo and in vitro perhaps by interfering with the NRF2-KEAP1 interaction

According to structure-based virtual screening using AutoDock, we found tiliroside may bind to KEAP1 by creating novel hydrogen bonding contacts within the protein's substrate binding cavity (Figure 1A). Figure 1B shows tiliroside at concentrations < 50 μM with no toxic effect on THLE-2 cells, but cell viability decreased significantly when the concentration was over 100 μM. The EC50 of tiliroside on THLE-2 cells after 24 hours was 155.9 μM. Next, we used qRT-PCR to examine the NRF2 and its transcriptional activation gene HO-1 mRNA expression levels in THLE-2 cells. The results demonstrated that, at doses below 5 μM, tiliroside treatment raised HO-1 expression in a concentration-dependent manner. Thus, 5 μM tiliroside was chosen for the next investigation (Figure 1C). However, NRF2 mRNA levels remained unchanged following tiliroside treatment (Figure 1C). Cellular thermal shift assay showed that tiliroside treatment significantly increased KEAP1's heat stability in THLE-2 cells (Figure 1D). Following tiliroside treatment, the KEAP1 protein's thermal melting curve obviously moved to the right (Figure 1D), suggesting that tiliroside may bind to KEAP1 in THLE-2 cells. Furthermore, co-immunoprecipitation was performed to examine any potential effects of tiliroside on the NRF2-KEAP1 interaction. According to our findings, tiliroside may interfere with NRF2-KEAP1 protein-protein interaction (PPI) (Figure 1E). In addition, 5 μM tiliroside treatment significantly abolished NRF2 destabilization in THLE-2 cells (Figure 1F), indicating that the degradation of NRF2 through ubiquitination was significantly inhibited by tiliroside treatment. Tiliroside treatment upregulated protein stability of NRF2 as shown by cycloheximide assay in THLE-2 cells (Figure 1G). Furthermore, tiliroside treatment significantly boosted NRF2's nuclear translocation and increased protein expression (Figure 1H). Furthermore, we assessed the potential of tiliroside therapy to activate NRF2 in hepatocytes in vivo. As the dose of tiliroside was raised, HO-1 mRNA levels progressively rose in comparison to those in the vehicle group, particularly in the group treated with tiliroside (20 mg/kg). However, HO-1 mRNA levels no longer increased after the tiliroside concentration was > 20 mg/kg (Figure 1I). Tiliroside treatment significantly activated NRF2 in mouse hepatocytes, as shown by the transcriptional activation of its downstream genes and a marked increase in NRF2 protein expression levels (Figures 1I–K). After tiliroside treatment, we analyzed the protein levels of NRF2

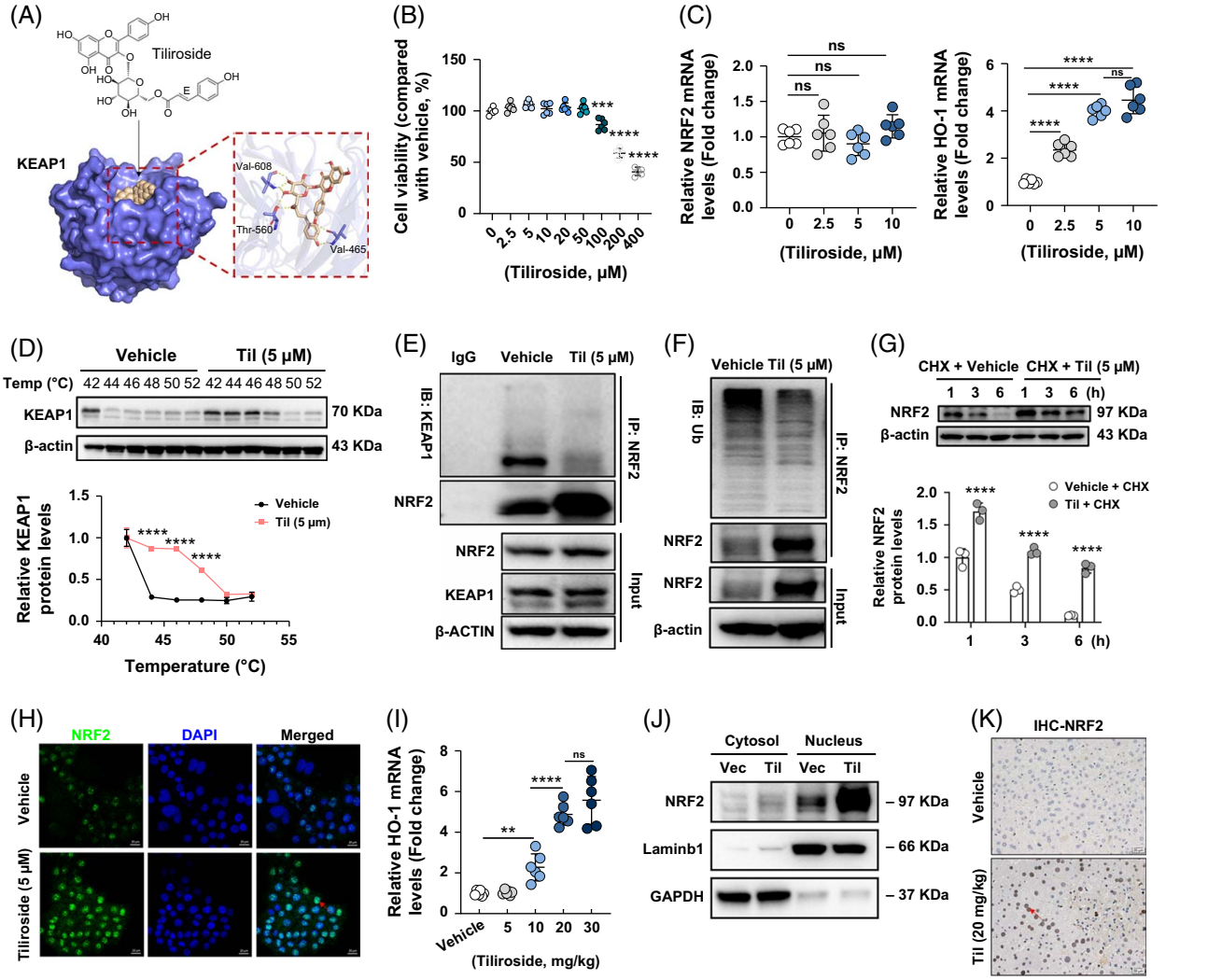

FIGURE 1 Tiliroside activated the NRF2/ARE pathway both in vivo and in vitro by disrupting the NRF2-KEAP1 interaction. (A) The molecular docking model predicted that the tiliroside binds to the Kelch domain of KEAP1. (B) A CCK8 assay was used to analyze the viability of THLE-2 cells treated with tiliroside in a concentration-dependent manner (2.5–400 μM) for 24 hours. (C) The mRNA levels of NRF2 and HO-1 in THLE-2 cells after treatment with different concentrations of tiliroside for 24 hours, as indicated. (D) CETSA of KEAP1 with or without tiliroside (5 μM) in THLE-2 cells. (E) THLE-2 cells were treated with 5 μM tiliroside for 24 hours and then immunoprecipitation was performed by using an NRF2 antibody, followed by a western blot analysis using anti-KEAP1 and NRF2 antibody. (F) THLE-2 cells were treated with 5 μM tiliroside for 24 hours and then treated with MG132 for 6 hours. Then, immunoprecipitation was performed by using an NRF2 antibody, followed by a western blot analysis using an anti-Ub antibody. (G) THLE-2 cells were treated with 20 μM CHX with or without 5 μM tiliroside for different times, then the protein levels of NRF2 were analyzed by western blot, and the quantification results were showed lower right. (H) Representative immunofluorescence staining for NRF2 in THLE-2 cells after treatment with 5 μM tiliroside for 24 hours (green: NRF2, blue: DAPI, scale bar: 20 μm, magnification ×400). (I) qRT-PCR was used to analyze the mRNA levels of HO-1 in mouse livers after daily gavage with vehicle or tiliroside (5, 10, 20, or 30 mg/kg/d) for 48 hours. (J) Western blot analysis of NRF2 subcellular localization in liver tissues after vehicle or tiliroside (20 mg/kg/d) treatment for 48 hours. (K) Immunohistochemical analysis of NRF2 expression in the livers of vehicle- or tiliroside-treated mice. The data are expressed as the mean ± SD of 3 independent experiments for cell experiments and 3 for animal experiments. ****$p < 0.0001$, ***$p < 0.001$, **$p < 0.01$ (1-way ANOVA). Abbreviations: CETSA, cellular thermal shift assay; CHX, cycloheximide; ns, not significant; Til, tiliroside.

target genes, including GCLC and HO-1. Our findings indicated a significant upregulation of HO-1 protein levels 1 hour after treatment, while GCLC protein levels were significantly elevated 3 hours after tiliroside administration (Supplemental Figures S1A–C, http://links.lww.com/HC9/B909). According to these findings, tiliroside may operate as an inhibitor of the KEAP1-NRF2 PPI to activate the NRF2/ARE signaling pathway.

Tiliroside protected against AILI in mice

The mice were gavaged with vehicle or tiliroside (20 mg/kg) daily 48 hours before APAP injection, as illustrated in Figure 2A. The results demonstrated that the tiliroside treatment at doses of 20 mg/kg/d and 30 mg/kg/d but not 10 mg/kg/d significantly reduced the levels of both ALT and AST (Figures 2B, C). Moreover, the administration of 30 mg/kg/d did not exhibit superior protective effects

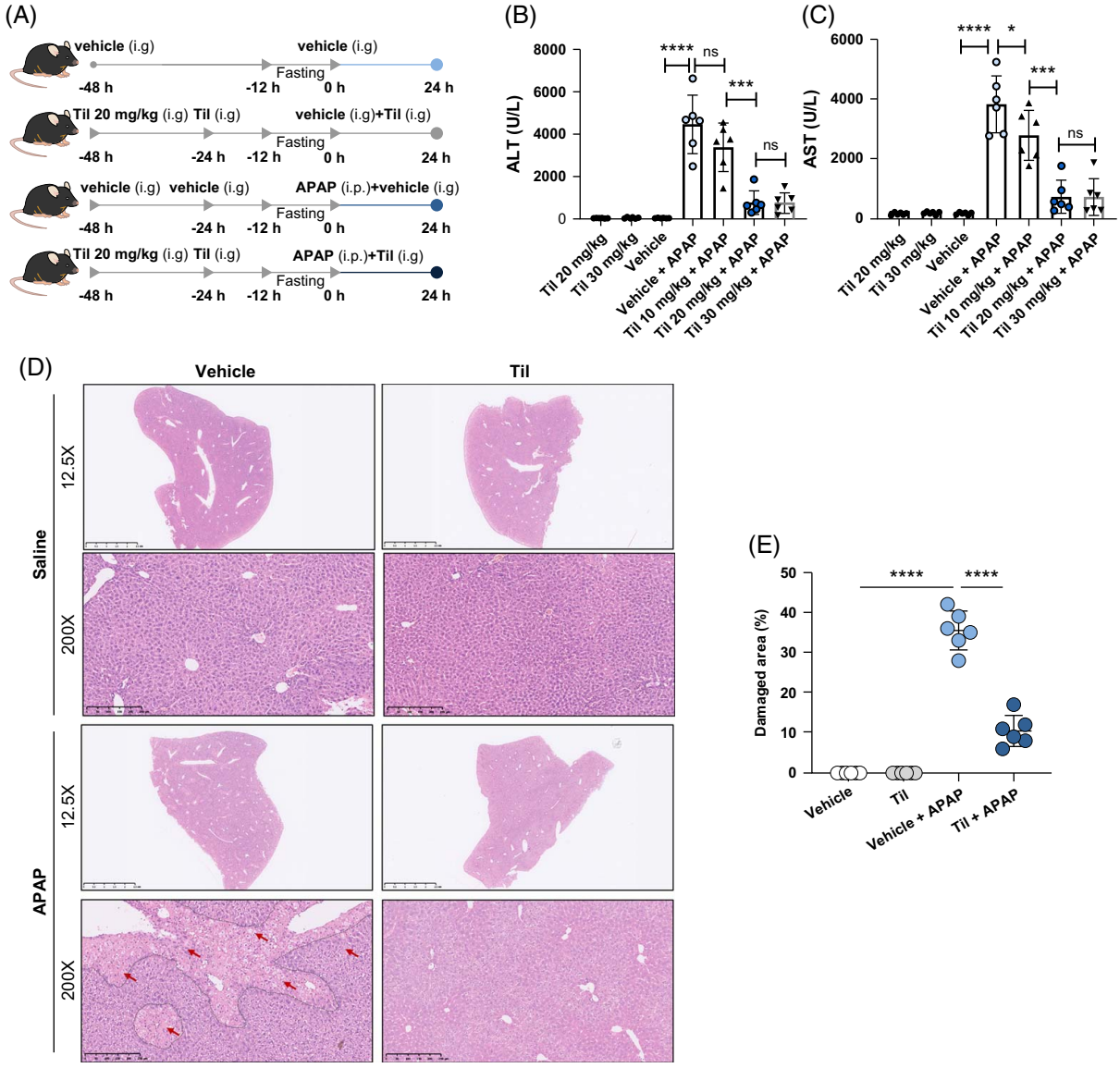

FIGURE 2 Tiliroside alleviated APAP-induced acute liver injury caused by hepatotoxicity in mice. (A) Animal treatment strategies. Mice were fasted for 12 hours after daily gavage of vehicle or tiliroside (20 mg/kg/d) for 48 hours. Then, the mice were injected intraperitoneally with APAP (400 mg/kg) and sacrificed 24 hours after APAP administration. Serum ALT (B) and AST (C) were detected in APAP-treated or control mice. (D) H&E staining of liver sections. Representative images showing necrotic areas in APAP-induced liver tissues treated with vehicle or tiliroside (magnification ×200; scale bar: 50 μm). (E) Quantitative analysis of the necrotic areas of the liver in (D). The data are expressed as the mean ± SD; n = 6 mice in each group; ****$p < 0.0001$, ***$p < 0.001$, *$p < 0.05$ (1-way ANOVA). Abbreviations: APAP, acetaminophen; ns, not significant; Til, tiliroside.

compared to 20 mg/kg/d; therefore, we selected the dosage of 20 mg/kg/d tiliroside for all animal models. The primary characteristic of APAP-induced hepatotoxicity, according to histological investigation, was the induction of significant hepatic centrilobular necrosis 24 hours after APAP treatment (Figure 2D). However, these effects improved after tiliroside (20 mg/kg/d) treatment, as indicated by a significant reduction in necrotic areas (Figures 2D, E).

Given that pretreatment with tiliroside is clinically irrelevant, we also administered tiliroside to the mice post-APAP injection at various time points. Our results indicated that tiliroside treatment (20 mg/kg) administered 3 and 6 hours after APAP injection had significant protective effects. However, these protective effects were markedly diminished when administered 9 hours after APAP injection (Supplemental Figures S2A, B, http://links.lww.com/HC9/B909). These results suggest tiliroside also has a therapeutic window after APAP injection. In addition, there was no obvious damage to the organs of normal mice after tiliroside (20 mg/kg) treatment for 1 month, indicating that tiliroside without obvious toxic side effects in normal mice (Supplemental Figures S2C–G, http://links.lww.com/HC9/B909). Taken together, these results showed that the hepatotoxicity caused by APAP was considerably reduced by tiliroside treatment.

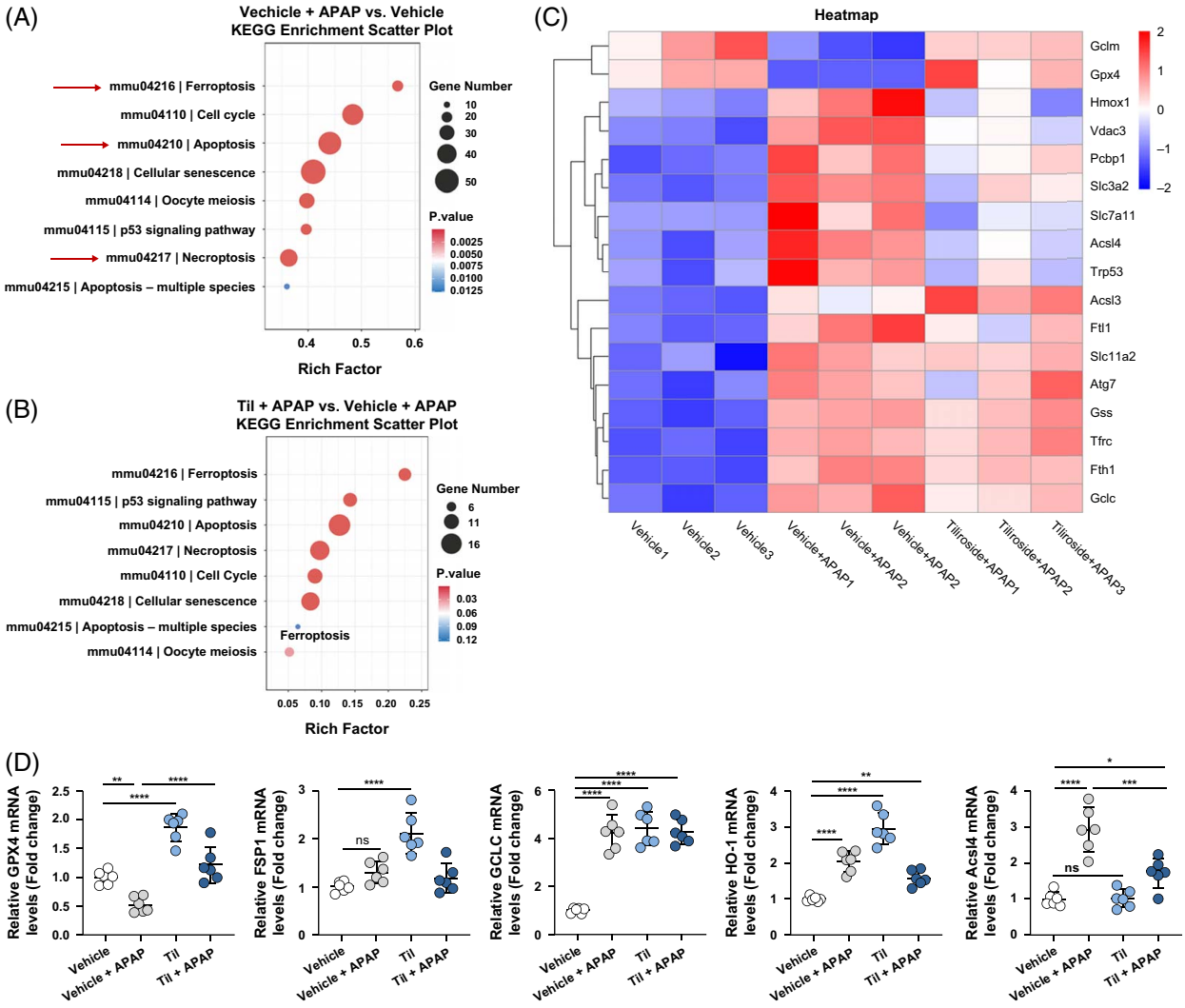

FIGURE 3 RNA-seq revealed that tiliroside treatment inhibited APAP-induced oxidative stress in hepatocytes. (A) KEGG enrichment analysis of the DEGs between the APAP and vehicle groups shows that genes involved in ferroptosis, apoptosis, and necroptosis signaling (marked with red arrows) were strongly differentially expressed after APAP treatment. (B) KEGG enrichment scatter plot showing the top differentially expressed genes involved in ferroptosis, apoptosis, and necroptosis (marked with red arrows) between the APAP + Til and APAP + vehicle groups. (C) Heatmap image showing the DEGs related to oxidative stress signaling in the vehicle, APAP, and APAP + Til groups. (D) The mRNA levels of GPX4, HO-1, GCLC, FSP1, and ACSL4 were also analyzed using qRT-PCR. The data are expressed as the mean ± SD; n = 3 for each group in the RNA-seq assay and n = 6 for each group in the qRT-PCR assay. ****$p < 0.0001$, ***$p < 0.001$, **$p < 0.01$ (1-way ANOVA). Abbreviations: APAP, acetaminophen, 400 mg/kg; DEG, differentially expressed gene; KEGG, Kyoto Encyclopedia of Genes and Genomes; Til, tiliroside, 20 mg/kg.

RNA-seq revealed that tiliroside treatment prevented APAP-induced oxidative stress in hepatocytes

RNA-seq was used to investigate potential protective mechanisms of tiliroside in AILI. A total of 9 liver samples from 3 groups were sequenced: the vehicle group, vehicle + APAP group, and tiliroside + APAP group. Gene expression levels in several groups were analyzed. Our results showed that there was a difference in the expression of ferroptosis, apoptosis, and necrosis-related genes in the APAP + vehicle group when compared to the vehicle group (Figure 3A). Comparably, the APAP + tiliroside group also showed notable alterations in ferroptosis, apoptosis, and necrosis-related pathway genes (Figure 3B). Tiliroside has the potential to function as an NRF2 activator, and NRF2 plays a key role in protecting against oxidative stress, so we focus on oxidative stress–related signaling pathways. The results of the heatmap analysis of the oxidative stress–related signaling pathway indicated that APAP significantly increased the expression of positive oxidative stress regulators, like ACSL4, while decreasing the expression of negative regulators, like glutathione peroxidase 4 (GPX4). These effects were nearly the opposite in the group that received tiliroside plus APAP (Figure 3C). The mRNA levels of several NRF2 target genes, including GPX4, HO-1, GCLC, and FSP1, were also analyzed using qRT-PCR. Our results indicate that tiliroside treatment upregulated the expression levels of GPX4, HO-1, GCLC,

and FSP1 while inhibiting the high levels of ACSL4 induced by APAP in the livers of mice (Figure 3D). All these results suggest tiliroside treatment prevented APAP-induced oxidative stress in hepatocytes.

Hepatocytes were protected by tiliroside against APAP-induced oxidative stress injury in vivo

In the mice livers treated with APAP, several oxidative stress markers were examined to determine whether tiliroside treatment might prevent APAP-induced hepatocyte oxidative stress injury in mice. Immunohistochemical staining revealed that APAP treatment markedly reduced the protein levels of GPX4, which was notably restored after tiliroside treatment (Figure 4A). Next, we used the oxidative stress marker myeloperoxidase (MPO) and the lipid peroxidation marker 4-hydroxynonenal (4-HNE) to examine APAP-induced oxidative damage in mice liver tissues. Histological analysis revealed that APAP significantly induced excessive accumulation of 4-HNE in the liver, which was then dramatically reduced by tiliroside treatment (Figure 4B). Similarly, tiliroside therapy significantly reduced APAP-induced MPO overaccumulation in the liver, according to western blot data (Figures 4C, D). We next measured the MDA levels and the GSH/GSSG ratios in mice livers to detect lipid peroxidation and oxidative stress. The findings showed that tiliroside therapy restored APAP-induced reductions in the GSH/GSSG ratio (Figure 4F) and significantly reduced APAP-induced increases in MDA levels (Figure 4E). Oxidative

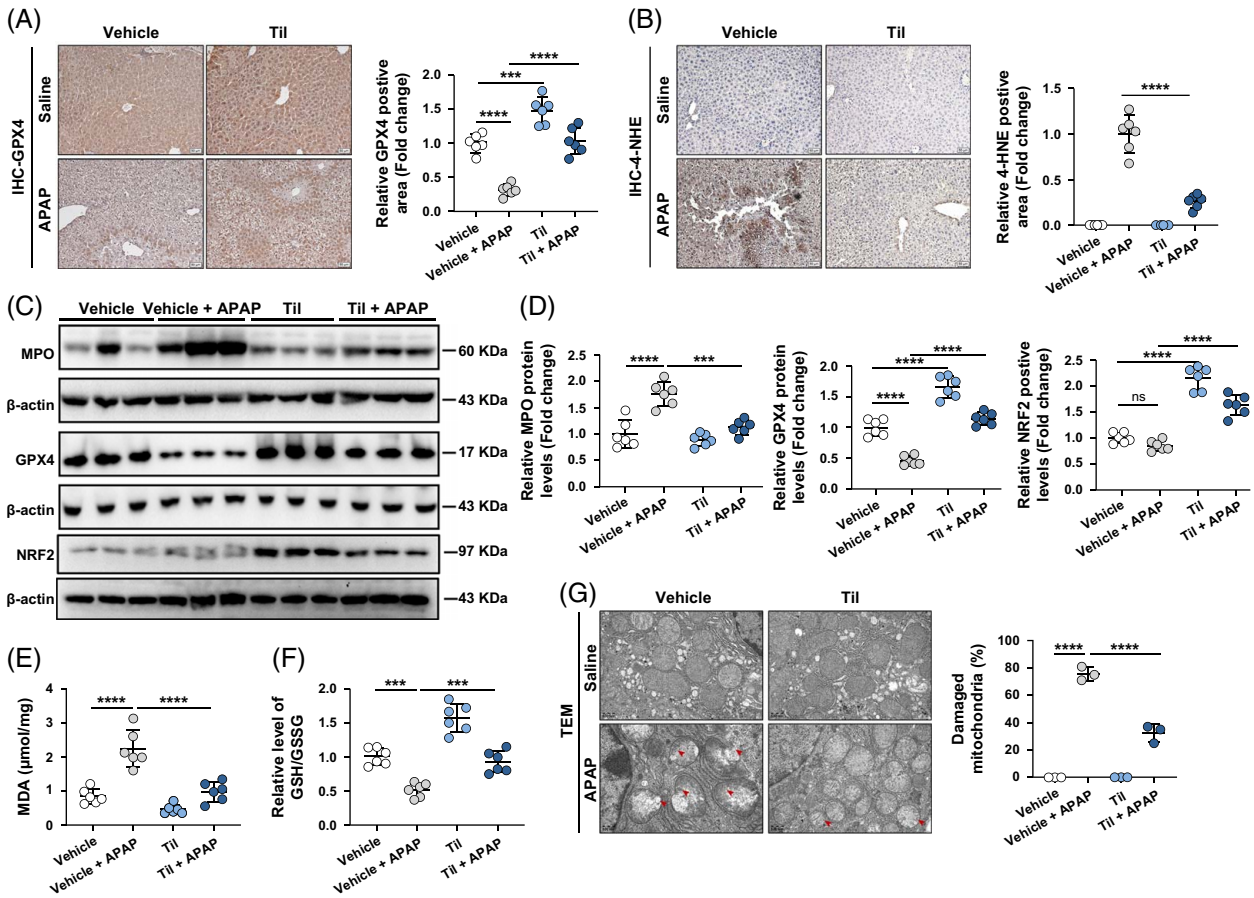

FIGURE 4 Tiliroside protected hepatocytes from APAP-induced oxidative stress in vivo. (A) The expression levels of GPX4 in the APAP-induced livers of all groups were detected by IHC (scale bar: 20 μm, magnification ×400), and the graph on the right side displays the relative quantitative results for GPX4. (B) Representative IHC image of 4-HNE in APAP-induced livers from mice treated with vehicle, vehicle + APAP, Til or Til + APAP (scale bar: 20 μm, magnification ×400). The relative quantified results are shown on the right. (C) Detection of MPO, GPX4, and NRF2 expression in the livers of mice after vehicle, APAP (300 mg/kg), tiliroside (20 mg/kg), or APAP combined with tiliroside treatment by western blot analysis; the quantitation results analyzed by ImageJ are shown on the right (D). (E) The MDA levels in the livers of mice after APAP or tiliroside treatment were determined by the MDA assay. (F) The relative ratio of GSH/GSSG (compared to that in the vehicle group) in the livers of mice treated with or without tiliroside (20 mg/kg) was measured with a GSH/GSSG kit. (G) APAP-induced mitochondrial damage in liver cells of mice treated with or without tiliroside (20 mg/kg) was observed using TEM. The red arrow indicates damaged mitochondria (scale bar: 1 μm). The data are expressed as the mean ± SD; n = 6 or 3 mice in each group. ****$p < 0.0001$, ***$p < 0.001$ (1-way ANOVA). Abbreviations: 4-HNE, 4-hydroxynonenal; APAP, acetaminophen; GSH, glutathione; GSSG, glutathione disulfide; IHC, immunohistochemistry; MDA, malondialdehyde; TEM, transmission electron microscopy; Til, tiliroside.

stress injury is often accompanied by dysregulation of mitochondrial morphology and function. Transmission electron microscopy analysis revealed severe mitochondrial damage in hepatocytes after the APAP challenge, characterized by increased mitochondrial rupture and decreased or no mitochondrial cristae. Notably, tiliroside treatment markedly ameliorated APAP-induced mitochondrial damage in hepatocytes (Figure 4G). These results suggest that APAP significantly inhibited APAP-induced hepatocyte oxidative stress injury in vivo.

Tiliroside treatment decreased APAP-induced hepatic cell death and inflammation in vivo

RNA-seq revealed that tiliroside treatment also inhibited APAP-induced cell death including ferroptosis, apoptosis, and necrosis in mouse livers. Terminal deoxynucleotidyl transferase-mediated dUTP nick-end labeling (TUNEL) staining was done to detect APAP-induced cell death in vivo. The number of TUNEL-positive cells in the livers of mice treated with APAP increased significantly, as seen in Figure 5A, but dropped significantly following treatment with tiliroside (Figure 5B). Furthermore, another significant pathological feature of APAP-induced hepatotoxicity is inflammation. Analysis was also done on APAP-induced hepatic inflammation in mice. The findings demonstrated that tiliroside administration considerably reduced the infiltration of APAP-induced hepatic macrophages in mice (Figures 5C, D). Furthermore, qRT-PCR was performed to detect the expression of inflammatory genes in mouse livers, including MCP-1, IL-1β, TNFα, and IL-6. The findings demonstrated that tiliroside administration dramatically reduced the levels of APAP-induced elevations in MCP-1, IL-1β, TNFα, and IL-6 in the mice's livers (Figure 5E).

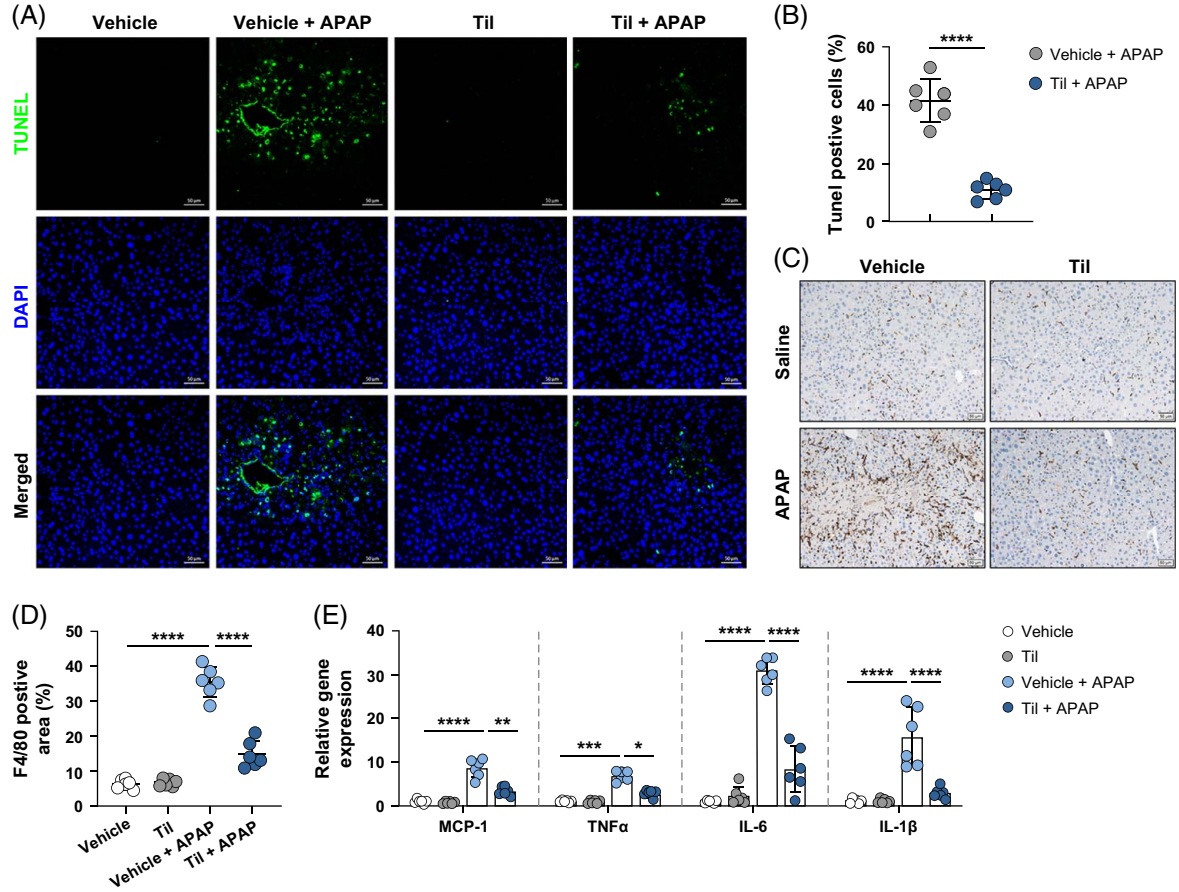

FIGURE 5 Tiliroside treatment ameliorated APAP-induced hepatic cell death and inflammation in vivo. (A) A TUNEL assay was used to analyze APAP-induced liver cell death in mice treated with vehicle, vehicle + APAP, Til or Til + APAP (green: TUNEL, blue: DAPI; scale bar: 20 μm; magnification: ×400). The number of TUNEL-positive cells in each group was calculated from 5 random fields in each sample, and the results are shown on the right (B). (C) Immunohistochemical staining of F4/80 in APAP-induced livers from mice treated with vehicle, vehicle + APAP, Til or Til + APAP (scale bar: 20 μm, magnification ×400); the graph shows the quantitative results (D). (E) QRT-PCR was used to analyze the mRNA levels of inflammatory genes, including MCP-1, TNF-α, IL-6, and IL-1β, in the livers of APAP-induced acute liver injury model mice treated with or without tiliroside (20 mg/kg). The data are expressed as the mean ± SD; n = 6 mice in each group. ****$p < 0.0001$, ***$p < 0.001$, **$p < 0.01$, *$p < 0.05$ (1-way ANOVA for B, D, 2-way ANOVA for E). Abbreviations: APAP, acetaminophen; Til, tiliroside; TUNEL, terminal deoxynucleotidyl transferase-mediated dUTP nick-end labeling.

Consequently, we concluded that tiliroside significantly ameliorated APAP-induced hepatocyte death and the inflammatory response in vivo.

Tiliroside's hepatoprotective effects were mediated by NRF2 in vivo

Next, we investigated if tiliroside's hepatoprotective effects in vivo were mediated by NRF2. We used hepatocyte-specific Cas9 transgenic mice (Alb-Cre$^+$ Cas9$^+$) to create hepatocyte-specific NRF2 KO animals to examine the effect of NRF2 deletion (KO) on the hepatoprotective effects of tiliroside in vivo. A schematic depicting the generation of Alb-Cre$^+$ Cas9$^+$ transgenic mice is shown in Figure 6A. PCR analysis revealed the genotyping results of the Alb-Cre$^+$ Cas9$^+$ offspring (Figure 6B). The western blot results indicated that we successfully constructed hepatocyte-specific Cas9 transgenic mice (Figure 6C). Figures 6D, E show that successful hepatocyte-specific NRF2 knockout mice were generated. In terms of body weight and organ functioning, the phenotypes of wild-type and hepatocyte-specific NRF2 knockout mice were similar (Figure 6F). Hepatocyte-specific NRF2 KO mice (NRF2 $^{Hep\ KO}$) that were subjected to AILI modeling were used to evaluate whether NRF2 mediated the hepatoprotective effects of tiliroside. After stimulation with APAP, NRF2 mutant animals had higher levels of ALT and AST than control mice, and this difference was not reversed by tiliroside intervention (Figures 7A, B). Like this, APAP stimulation significantly changed the liver pathology of NRF2 knockout mice; in contrast, the liver pathology of mice in the NRF2 $^{Hep\ KO}$ tiliroside + APAP group was not significantly different from that of the NRF2 $^{Hep\ KO}$ + APAP group (Figures 7C, D). By examining liver oxidative stress indices in mice, the study revealed that the protective effect of tiliroside against APAP-induced oxidative stress and acute liver damage was removed by hepatocyte-specific deletion of NRF2. Furthermore, hepatocyte-specific NRF2 deletion abolished tiliroside's capacity to reduce oxidative stress and APAP-induced hepatocyte damage, according to the results of the MDA and 4-HNE expression experiments (Figures 7E–G). In the livers of NRF2 $^{Hep\ KO}$ mice, tiliroside therapy was unable to raise GPX4 expression or lower APAP-induced MPO levels (Figures 7H, I). These findings imply that NRF2 mediates the protective effects of tiliroside against AILI.

Tiliroside prevented APAP-induced oxidative stress in cultured human hepatocytes in vitro

The protective effects of tiliroside on human THLE-2 cells were also examined to detect whether the drug directly inhibits APAP-induced oxidative stress of hepatocytes. The CCK8 assay demonstrated that APAP treatment induced more than half of the THLE-2 cell death, but the cell viability was reversed to more than 75% after treatment with tiliroside (Figure 8A). In addition, tiliroside treatment markedly decreased APAP-induced increases in MDA levels in THLE-2 cells (Figure 8B). Other features of oxidative stress, including lipid peroxidation and mitochondrial damage, were also analyzed. We applied BODIPY 581/591 C11 to detect the protective effect of tiliroside against lipid peroxidation in THLE-2 cells. Following APAP treatment, as demonstrated in Figure 8C, the fluorescence of the BODIPY 581/591 C11 probe changed from red to green, indicating that APAP promoted lipid peroxidation in THLE-2 cells. Tiliroside treatment greatly blunted APAP-induced lipid peroxidation in THLE-2 cells (Figure 8C). In addition, we stained the cells with MitoSOX Red and TMRM fluorescent probes to detect APAP-induced mitochondrial ROS accumulation and depolarization of mitochondrial membrane potential. The findings showed that, in THLE-2 cells, tiliroside treatment led to a significant decrease in mitochondrial ROS levels, but APAP therapy caused a notable rise in ROS levels after 24 hours (Figure 8D). Tiloroside therapy also dramatically restored the mitochondrial membrane potential depolarization caused by APAP in THLE-2 cells, as demonstrated in Figure 8E. These findings suggested that tiliroside therapy significantly improved the mitochondrial damage caused by APAP in THLE-2 cells. Furthermore, our findings indicated that both GCLC and HO-1 play an equally crucial role in the protective effects of tiliroside on APAP-induced THLE-2 cells. This was demonstrated by employing DL-Buthionine-(S, R)-sulfoximine (BSO) to inhibit GSH synthesis and HO-1-IN1 to inhibit HO-1 (Supplemental Figure S3, http://links.lww.com/HC9/B909). Using CRISPR/Cas9 methods, we produced NRF2 knockout THLE-2 cells (NRF2 KO) to find out if NRF2 mediated tiliroside's hepatocyte-protective effects. NRF2 KO cells were successfully generated, according to western blot results (Figure 8F). The CCK8 and western blot results showed that NRF2 deletion significantly reduced tiliroside's hepatocyte-protective effects. There was no appreciable difference in the viability of the cells (Figure 8G) or GPX4 protein levels (Figure 8H) between APAP-treated NRF2 KO cells with or without tiliroside therapy. In summary, tiliroside treatment inhibited APAP-induced oxidative stress in cultured human hepatocytes by activating NRF2.

DISCUSSION

One of the primary pathogenic processes causing AILI is oxidative stress, and it has been shown that target oxidative stress is useful in reducing AILI.[8,10] The

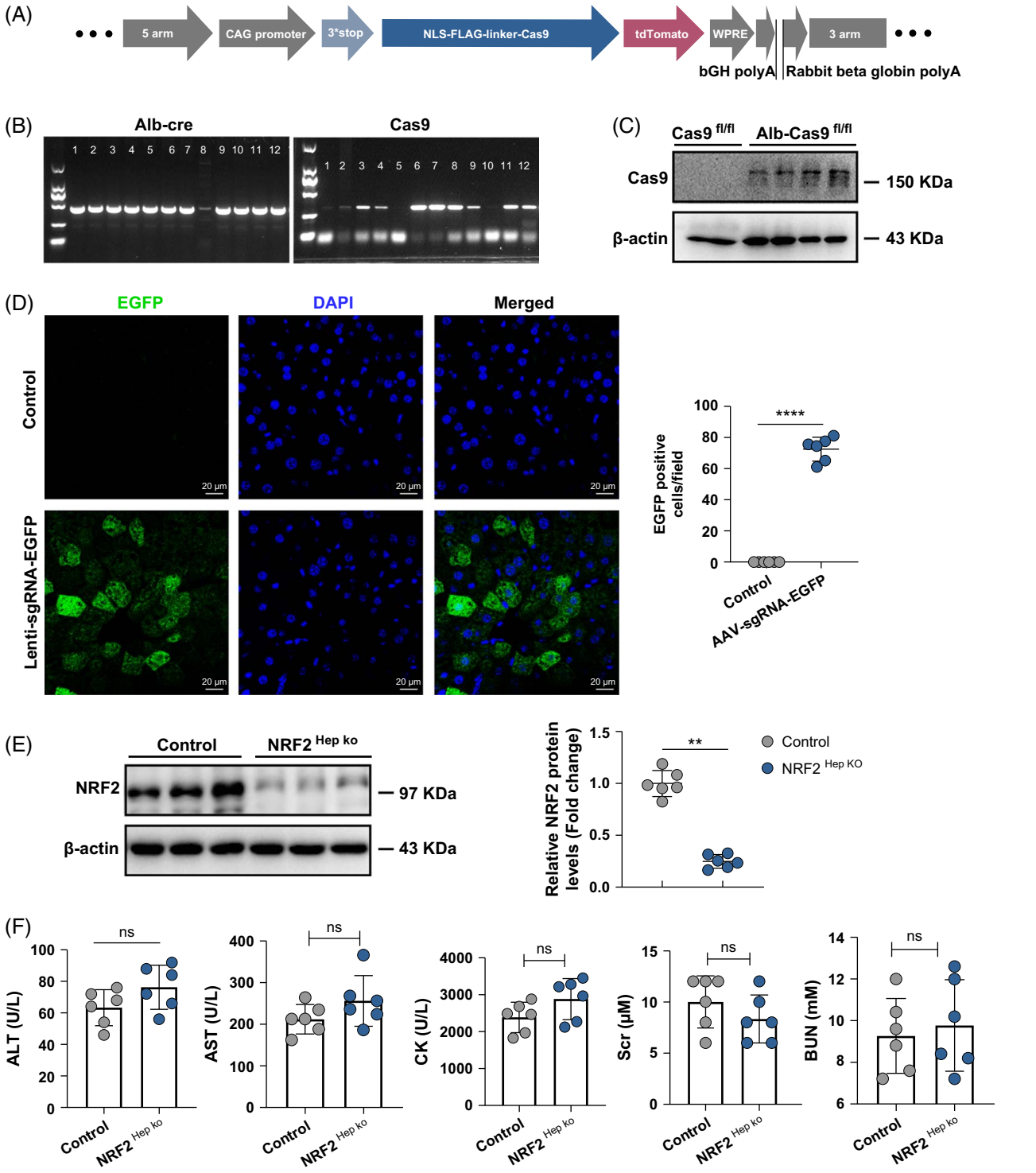

FIGURE 6 The construction of liver-specific NRF2 knockout mice. (A) Schematic depicting the generation of CRISPR/cas9 knock-in mice. (B) PCR analysis was used to genotype the Alb-Cre$^+$ Cas9$^+$ offspring. (C) Western blot analysis of the Cas9 protein expression levels in the livers of Cas9$^+$ and Alb-Cre$^+$ Cas9$^+$ mice. (D) EGFP immunofluorescence analysis of EGFP expression in the livers of mice injected with Lenti-NRF2-sgRNA-EGFP or control (green: EGFP, blue: DAPI, scale bar: 20 μm, magnification ×400), and the graph on the right side displayed the relative quantitative results for EGFP. (E) NRF2 protein levels of livers in Alb-Cre$^+$ Cas9$^+$ mice injected with Lenti-NRF2-sgRNA-EGFP or control were determined by western blot, and the graphs on the right showed the results of densitometry analysis performed by ImageJ. (F) Measurements of plasma biochemical parameters for the liver (ALT, AST), kidney (BUN, SCr), and heart functions (CK, creatine kinase) after the mice injected with Lenti-NRF2-sgRNA-EGFP or control. Data are expressed as the mean ± SD, n = 6 mice of each group. ****$p < 0.0001$, **$p < 0.01$, ns: not significant.

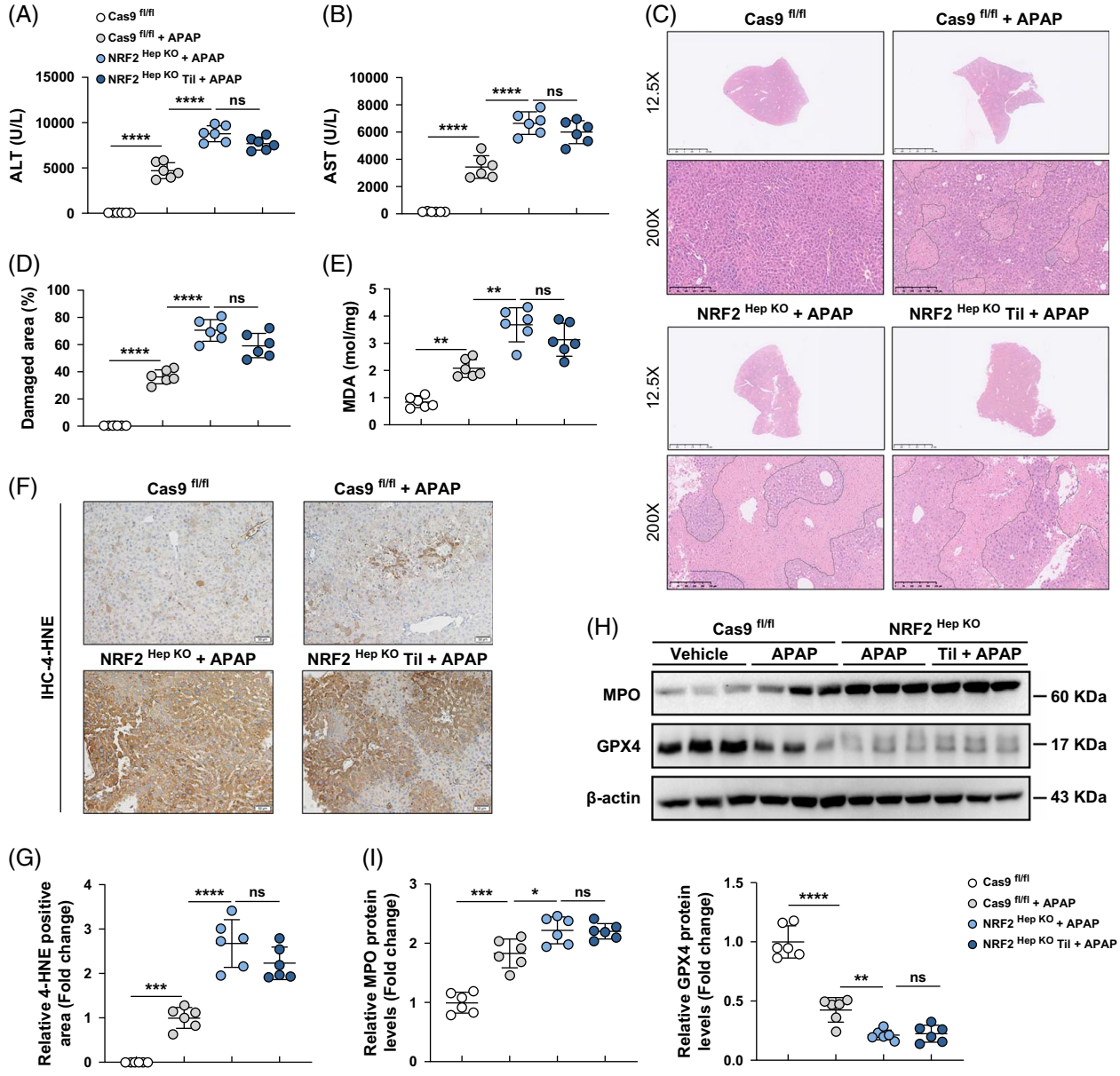

FIGURE 7 NRF2-mediated hepatoprotective effects of tiliroside in vivo. ALT (A) and AST (B) levels in APAP-treated (400 mg/kg) control mice or NRF2 $^{Hep\ KO}$ mice treated with or without tiliroside (20 mg/kg). (C) H&E staining of livers from APAP-induced control mice or NRF2 $^{Hep\ KO}$ mice treated with or without tiliroside (20 mg/kg) (magnification ×200; scale bar: 50 μm). (D) Quantitative analysis of the necrotic areas of the liver in (C). (E) MDA levels in APAP-induced livers from control mice or NRF2 $^{Hep\ KO}$ mice treated with or without tiliroside. (F) Representative 4-HNE IHC images of APAP-induced livers from control mice or NRF2 $^{Hep\ KO}$ mice treated with or without tiliroside (scale bar: 20 μm, magnification ×400). (G) The relative quantified results of (F). (H) Western blot analysis of the MPO and GPX4 protein levels in the livers of APAP-induced control mice or NRF2 $^{Hep\ KO}$ mice treated with or without tiliroside, the quantitation results analyzed by ImageJ are shown on the down (I). ****$p < 0.0001$, ***$p < 0.001$, **$p < 0.01$ (1-way ANOVA). ns, not significant. The data are expressed as the mean ± SD of 6 or 3 mice in each group. Abbreviations: 4-HNE, 4-hydroxynonenal; APAP, acetaminophen; IHC, immunohistochemistry; MDA, malondialdehyde.

NRF2/KEAP1 pathway is one of the key defense mechanisms against APAP-induced oxidative stress in hepatocytes,[18,32] which is crucial for preventing oxidative and pro-electrophilic stress as well as for maintaining the cellular redox status.[14,33] Downstream target genes of NRF2, GPX4, GCLC, and HO-1 are the key enzymes identified to directly reduce oxidative stress.[34,35] KEAP1 mediates the ubiquitin-degradation of NRF2 by attaching to it. As a result, breaking the PPI between NRF2 and KEAP1 has become a very promising method of activating NRF2 to cure a variety of oxidative stress–related illnesses.[36,37] However, no inhibitors of the NRF2-KEAP1 PPI have been translated into the clinic for side effects or other reasons.

Our attention was attracted to natural substances derived from plants that have anti-inflammatory and antioxidant properties, such as Chinese herbal remedies. For centuries, the dried fruits of oriental paper

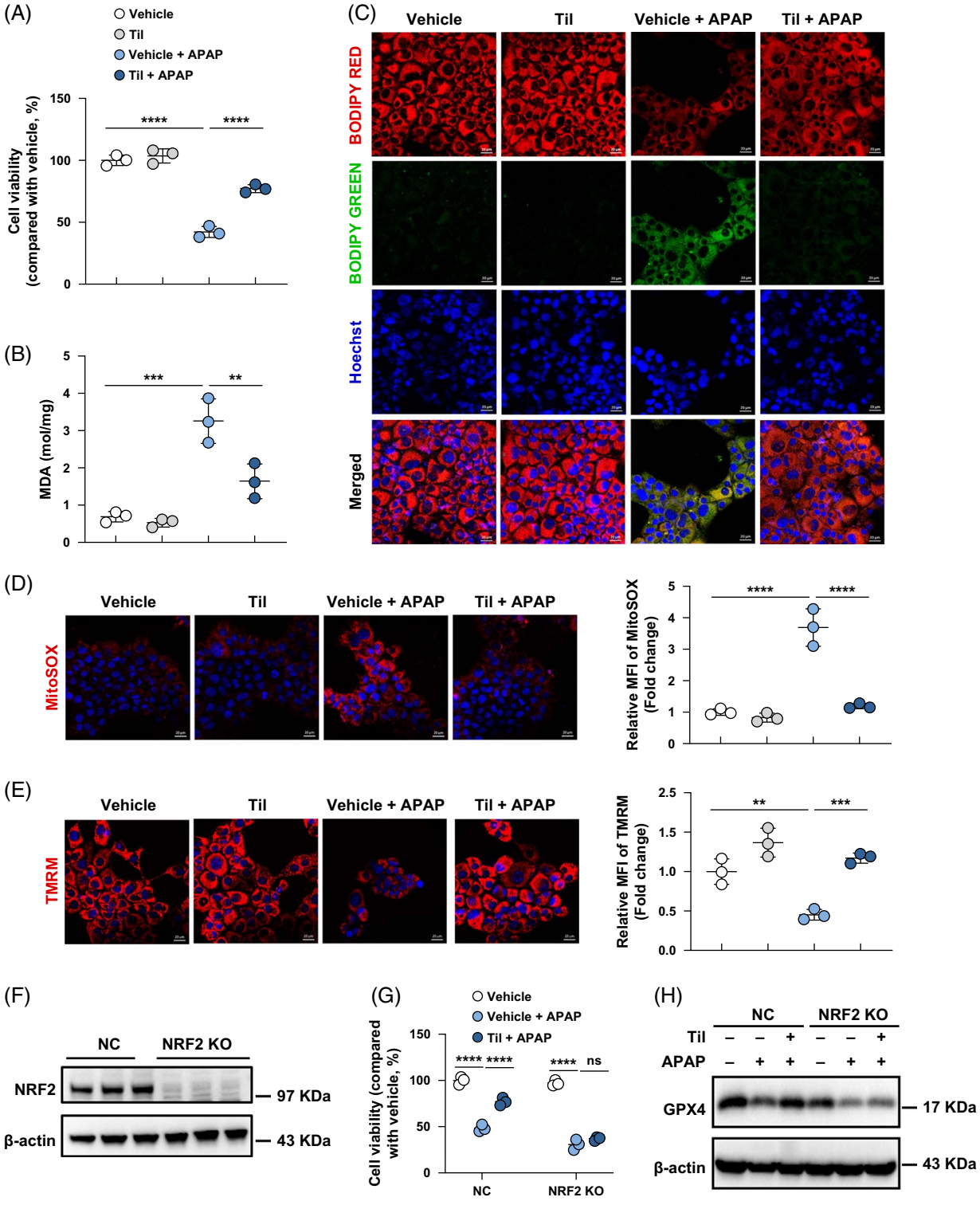

FIGURE 8 Tiliroside prevented APAP-induced oxidative stress in cultured human hepatocytes. THLE-2 cells were incubated with APAP (10 mM) or tiliroside (5 μM) for 24 hours. Cell viability was measured by a CCK8 assay (A), and the levels of MDA were determined by an MDA assay (B). (C) Lipid peroxidation in THLE-2 cells induced by APAP (10 μg/mL, 24 h) and treated with or without tiliroside (5 μM) for 24 hours was analyzed by staining with fluorescent lipophilic BODIPY 581/591 C11 probe (red: total lipids, green: oxidized lipids, blue: Hoechst, scale bar: 20 μm) and captured by confocal fluorescence microscopy. (D) MitoSOX Red staining was used to detect mitochondrial ROS accumulation in THLE-2 cells (red: MitoSOX; blue: Hoechst; scale bar: 20 μm), and the graph of the relative quantitative results is displayed on the right. (E) Changes in the mitochondrial membrane potential of THLE-2 cells induced by APAP (10 mM, 24 h) and treated with or without tiliroside (5 μM) for 24 hours were analyzed by staining with TMRM fluorescent probes (red: TMRM; blue: Hoechst; scale bar: 20 μm), and a graph of the relative quantitative results is displayed on the right. (F) Detection of NRF2 expression levels in NC and NRF2-KO THLE-2 cells by western blot analysis.

(G) A CCK8 assay was used to determine the viability of NC and NRF2-KO cells treated with vehicle, APAP (10 mM), or tiliroside (5 μM) for 24 hours. (H) NC and NRF2-KO cells were treated with APAP (10 mM, 24 h) combined with or without tiliroside (5 μM). The expression levels of GPX4 were detected by western blot analysis. ****$p < 0.0001$, ***$p < 0.001$, **$p < 0.01$ (1-way ANOVA for A, B, D, E; 2-way ANOVA for G). ns, not significant. The data are expressed as the mean ± SD of 3 independent experiments. Abbreviations: APAP, acetaminophen; MDA, malondialdehyde.

bush flowers have been used as a natural remedy for maintaining health and combating various diseases.[38] Numerous studies have shown that tiliroside, a primary constituent and powerful natural flavonoid glycoside of oriental paper bush flowers, possesses a range of pharmacological actions, such as antipyretic, anti-inflammatory, as well as antioxidant properties.[39,40] Prior research has demonstrated that tiliroside and its derivatives can activate NRF2 to produce neuroprotective effects; however, it is still unknown how precisely tiliroside works. Based on functional studies and molecular docking patterns, our research suggests tiliroside may bind to KEAP1 and disrupt the NRF2-KEAP1 PPI, hence activating NRF2 in hepatocytes.

Furthermore, our findings showed that AILI was considerably improved by tiliroside therapy, both in vivo and in vitro. RNA-seq results revealed that APAP-treated mice exhibited aberrant ferroptosis, apoptosis, and necrotic cell death. Fortunately, tiliroside markedly reversed the APAP-induced abnormalities in these processes. Analysis revealed tiliroside improved abnormalities in several oxidative stress indicators by APAP, including GPX4 and MPO protein levels, 4-HNE and MDA levels, GSH/GSSG ratios, and mitochondrial damage, and demonstrated that tiliroside treatment dramatically ameliorated hepatocyte oxidative stress in AILI mice. Furthermore, no significant damage to the organs of normal mice was observed following 1 month of treatment with tiliroside (20 mg/kg). This suggests that tiliroside may also have the potential to alleviate chronic liver damage. In addition, hepatocyte-specific NRF2 knockout mice exhibited more severe liver injury induced by APAP, which could not be improved by tiliroside treatment, suggesting that tiliroside's hepatoprotective effects were mediated by NRF2. Similarly, tiliroside has a direct antioxidative stress effect on cultured human hepatocyte THLE-2 cells. Furthermore, the hepatoprotective effects of tiliroside on THLE-2 cells were significantly attenuated by NRF2 deletion. Our results indicate that tiliroside may be a KEAP1-NRF2 PPI inhibitor, indicating that it is a useful strategy to find potential NRF2-KEAP1 PPI inhibitors from natural substances. Furthermore, most natural substances have few adverse effects as most of them come from edible plants or other organisms. Tiliroside inhibited NRF2 ubiquitination-mediated degradation, suggesting that it may be an inhibitor of the KEAP1-NRF2 PPI. However, the direct interactions between KEAP1 and tiliroside need further research. Furthermore, a recent study found that by inhibiting TBK1, tiliroside therapy could cause ferroptosis in cancer cells.[41]. Our results and those of previous studies suggest that tiliroside has different effects on normal and tumor cells. In addition, our results indicated that tiliroside treatment at higher doses (> 100 μM) could induce cell death in vitro, suggesting that the translation of tiliroside to clinical applications requires further investigation. Although the detailed mechanisms by which tiliroside mediates different pharmacological effects and its clinical safety need further study, our research showed that tiliroside could prevent AILI perhaps through disrupting KEAP1-NRF2 PPI and activating NRF2.

CONCLUSIONS

In summary, our results suggest that tiliroside could be used as a possible NRF2 activator to protect against APAP-induced hepatocyte ferroptosis and suggest that tiliroside can be developed as a potential hepatoprotective drug in the clinic.

DATA AVAILABILITY STATEMENT

All the data are available from the corresponding authors upon reasonable request. The RNA-sequencing data of mouse livers were submitted to the NCBI SRA database under accession number PRJNA1017907.

AUTHOR CONTRIBUTIONS

Fangfang Cai: writing—original draft, project administration, methodology, investigation, data curation, and conceptualization. Kaiqian Zhou: methodology and investigation. Peipei Wang: methodology and data curation. Wen Zhang: visualization and data curation. Lei Liu: investigation. Yunwen Yang: writing—review and editing, supervision, funding acquisition, conceptualization, and data curation. All authors have read and approved the final version of this manuscript.

FUNDING INFORMATION

This work was supported by the National Natural Science Foundation of China (grant. no. 82400816 and 82370683), the Natural Science Foundation of Jiangsu Province (grant. no. BK20221034), the China Postdoctoral Science Foundation (2022M723505), Nanjing Health Science and Technology Development Foundation (ZKX22049), and the Natural Science basic research program of Shaanxi Province (2023-JC-QN-0873).

CONFLICTS OF INTEREST

The authors have no conflicts to report.

ETHICAL APPROVAL

All animal welfare and experimental procedures were approved by the Institutional Animal Care and Use Committee of Nanjing Medical University.

ORCID

Yunwen Yang https://orcid.org/0000–0002–1916–5716

REFERENCES

1. Horvatits T, Drolz A, Trauner M, Fuhrmann V. Liver injury and failure in critical illness. Hepatology. 2019;70:2204–15.
2. McGill MR, Sharpe MR, Williams CD, Taha M, Curry SC, Jaeschke H. The mechanism underlying acetaminophen-induced hepatotoxicity in humans and mice involves mitochondrial damage and nuclear DNA fragmentation. J Clin Invest. 2012;122:1574–83.
3. Dahlin DC, Miwa GT, Lu AY, Nelson SD. N-acetyl-p-benzoquinone imine: A cytochrome P-450-mediated oxidation product of acetaminophen. Proc Natl Acad Sci USA. 1984;81:1327–31.
4. Ni HM, McGill MR, Chao X, Du K, Williams JA, Xie Y, et al. Removal of acetaminophen protein adducts by autophagy protects against acetaminophen-induced liver injury in mice. J Hepatol. 2016;65:354–62.
5. Reuben A, Tillman H, Fontana RJ, Davern T, McGuire B, Stravitz RT, et al. Outcomes in adults with acute liver failure between 1998 and 2013: An observational cohort study. Ann Intern Med. 2016;164:724–32.
6. Pakravan N, Waring WS, Sharma S, Ludlam C, Megson I, Bateman DN. Risk factors and mechanisms of anaphylactoid reactions to acetylcysteine in acetaminophen overdose. Clin Toxicol (Phila). 2008;46:697–702.
7. Jaeschke H, Akakpo JY, Umbaugh DS, Ramachandran A. Novel therapeutic approaches against acetaminophen-induced liver injury and acute liver failure. Toxicol Sci. 2020;174:159–67.
8. Yan M, Huo Y, Yin S, Hu H. Mechanisms of acetaminophen-induced liver injury and its implications for therapeutic interventions. Redox Biol. 2018;17:274–83.
9. Chowdhury A, Nabila J, Adelusi Temitope I, Wang S. Current etiological comprehension and therapeutic targets of acetaminophen-induced hepatotoxicity. Pharmacol Res. 2020;161:105102.
10. Du K, Ramachandran A, Jaeschke H. Oxidative stress during acetaminophen hepatotoxicity: Sources, pathophysiological role and therapeutic potential. Redox Biol. 2016;10:148–56.
11. Sun X, Ou Z, Chen R, Niu X, Chen D, Kang R, et al. Activation of the p62-Keap1-NRF2 pathway protects against ferroptosis in hepatocellular carcinoma cells. Hepatology. 2016;63:173–84.
12. Suzuki T, Motohashi H, Yamamoto M. Toward clinical application of the Keap1-Nrf2 pathway. Trends Pharmacol Sci. 2013;34:340–6.
13. Itoh K, Mimura J, Yamamoto M. Discovery of the negative regulator of Nrf2, Keap1: A historical overview. Antioxid Redox Signal. 2010;13:1665–78.
14. Bellezza I, Giambanco I, Minelli A, Donato R. Nrf2-Keap1 signaling in oxidative and reductive stress. Biochim Biophys Acta Mol Cell Res. 2018;1865:721–33.
15. Silva-Islas CA, Maldonado PD. Canonical and non-canonical mechanisms of Nrf2 activation. Pharmacol Res. 2018;134:92–9.
16. Li H, Weng Q, Gong S, Zhang W, Wang J, Huang Y, et al. Kaempferol prevents acetaminophen-induced liver injury by suppressing hepatocyte ferroptosis via Nrf2 pathway activation. Food Funct. 2023;14:1884–96.
17. Wang L, Zhang S, Cheng H, Lv H, Cheng G, Ci X. Nrf2-mediated liver protection by esculentoside A against acetaminophen toxicity through the AMPK/Akt/GSK3beta pathway. Free Radic Biol Med. 2016;101:401–12.
18. Cai C, Ma H, Peng J, Shen X, Zhen X, Yu C, et al. USP25 regulates KEAP1-NRF2 anti-oxidation axis and its inactivation protects acetaminophen-induced liver injury in male mice. Nat Commun. 2023;14:3648.
19. Subramanya SB, Venkataraman B, Meeran MFN, Goyal SN, Patil CR, Ojha S. Therapeutic potential of plants and plant derived phytochemicals against acetaminophen-induced liver injury. Int J Mol Sci. 2018;19:3776.
20. Zhang HY, Wang HL, Zhong GY, Zhu JX. Molecular mechanism and research progress on pharmacology of traditional Chinese medicine in liver injury. Pharm Biol. 2018;56:594–611.
21. Gao M, Yi J, Zhu J, Minikes AM, Monian P, Thompson CB, et al. Role of mitochondria in ferroptosis. Mol Cell. 2019;73:354–63 e3.
22. Chen Y, Zhang C, Jin MN, Qin N, Qiao W, Yue XL, et al. Flavonoid derivative exerts an antidiabetic effect via AMPK activation in diet-induced obesity mice. Nat Prod Res. 2016;30:1988–92.
23. Velagapudi R, Aderogba M, Olajide OA. Tiliroside, a dietary glycosidic flavonoid, inhibits TRAF-6/NF-kappaB/p38-mediated neuroinflammation in activated BV2 microglia. Biochim Biophys Acta. 2014;1840:3311–9.
24. Velagapudi R, El-Bakoush A, Olajide OA. Activation of Nrf2 pathway contributes to neuroprotection by the dietary flavonoid tiliroside. Mol Neurobiol. 2018;55:8103–23.
25. Velagapudi R, Jamshaid F, Lepiarz I, Katola FO, Hemming K, Olajide OA. The tiliroside derivative, 3-O-[(E)-(2-oxo-4-(p-tolyl) but-3-en-1-yl] kaempferol produced inhibition of neuroinflammation and activation of AMPK and Nrf2/HO-1 pathways in BV-2 microglia. Int Immunopharmacol. 2019;77:105951.
26. Cai F, Li D, Zhou K, Zhang W, Yang Y. Tiliroside attenuates acute kidney injury by inhibiting ferroptosis through the disruption of NRF2-KEAP1 interaction. Phytomedicine. 2024;126:155407.
27. Yang Y, Cai F, Zhou N, Liu S, Wang P, Zhang S, et al. Dimethyl fumarate prevents ferroptosis to attenuate acute kidney injury by acting on NRF2. Clin Transl Med. 2021;11:e382.
28. Gao H, Jin Z, Bandyopadhyay G, Wang G, Zhang D, Rocha KCE, et al. Aberrant iron distribution via hepatocyte-stellate cell axis drives liver lipogenesis and fibrosis. Cell Metab. 2022;34:1201–13 e5.
29. Cai F, Xu H, Cao N, Zhang X, Liu J, Lu Y, et al. ADT-OH, a hydrogen sulfide-releasing donor, induces apoptosis and inhibits the development of melanoma in vivo by upregulating FADD. Cell Death Dis. 2020;11:33.
30. Seneviratne U, Huang Z, Am Ende CW, Butler TW, Cleary L, Dresselhaus E, et al. Photoaffinity labeling and quantitative chemical proteomics identify LXRbeta as the functional target of enhancers of astrocytic apoE. Cell Chem Biol. 2021;28:148–57 e7.
31. Jensen EC. Quantitative analysis of histological staining and fluorescence using ImageJ. Anat Rec (Hoboken). 2013;296:378–81.
32. Li Q, Zhang W, Cheng N, Zhu Y, Li H, Zhang S, et al. Pectolinarigenin ameliorates acetaminophen-induced acute liver injury via attenuating oxidative stress and inflammatory response in Nrf2 and PPARa dependent manners. Phytomedicine. 2023;113:154726.
33. Wu T, Zhao F, Gao B, Tan C, Yagishita N, Nakajima T, et al. Hrd1 suppresses Nrf2-mediated cellular protection during liver cirrhosis. Genes Dev. 2014;28:708–22.
34. Qiu W, Zhang X, Pang X, Huang J, Zhou S, Wang R, et al. Asiatic acid alleviates LPS-induced acute kidney injury in broilers by inhibiting oxidative stress and ferroptosis via activation of the Nrf2 pathway. Food Chem Toxicol. 2022;170:113468.
35. Xie Y, Kang R, Klionsky DJ, Tang D. GPX4 in cell death, autophagy, and disease. Autophagy. 2023;19:2621–38.
36. Lee SM, Hu LQ. Nrf2 activation through the inhibition of Keap1-Nrf2 protein-protein interaction. Med Chem Res. 2020;29:846–67.

37. Crisman E, Duarte P, Dauden E, Cuadrado A, Rodriguez-Franco MI, Lopez MG, et al. KEAP1-NRF2 protein-protein interaction inhibitors: Design, pharmacological properties and therapeutic potential. Med Res Rev. 2023;43:237–87.
38. Wang DH, Wang MY, Shen WH, Yuan JF. Analysis of chemical compounds and toxicological evaluation of Forsythia suspensa leaves tea. Food Sci Biotechnol. 2021;30:305–14.
39. Calzada F, Basurto JC, Barbosa E, Velazquez C, Hernandez NG, Ordonez Razo RM, et al. Antiprotozoal activities of tiliroside and other compounds from Sphaeralcea angustifolia (Cav.) G. Don. Pharmacognosy Res. 2017;9:133–7.
40. Grochowski DM, Locatelli M, Granica S, Cacciagrano F, Tomczyk M. A review on the dietary flavonoid tiliroside. Compr Rev Food Sci Food Saf. 2018;17:1395–421.
41. Yang C, Lu T, Liu M, Yuan X, Li D, Zhang J, et al. Tiliroside targets TBK1 to induce ferroptosis and sensitize hepatocellular carcinoma to sorafenib. Phytomedicine. 2023;111:154668.

How to cite this article: Cai F, Zhou K, Wang P, Zhang W, Liu L, Yang Y. A novel KEAP1 inhibitor, tiliroside, activates NRF2 to protect against acetaminophen-induced oxidative stress and acute liver injury. Hepatol Commun. 2025;9: e0658. https://doi.org/10.1097/HC9.0000000000000658